Dedicated to Academician Aureliu Sandulescu's 80^{th} Anniversary

ALPHA-DECAY DATA OF SUPERHEAVY NUCLEI AS A SOURCE OF INFORMATION ABOUT NUCLEAR STATES

I. SILIŞTEANU[a], A. I. BUDACA

"Horia Hulubei" National Institute for Physics and Nuclear Engineering
30 Reactorului, Bucharest-Magurele, RO-077125, Romania
Email: [a]silist@theory.nipne.ro

Received January 10, 2012

Two different descriptions of α-decay rates, namely, microscopic shell-model approach and phenomenological description are emphasized to study the structure and dynamics of heaviest nuclei. On the structure side, improvements to nuclear models are being explored to take more accurately into account the role of the shell and pairing effects and importance of excitation and deformation. The accuracy of available experimental half-lives is discussed and a spectroscopic information is derived from the ratio of theoretical to experimental results. The universality of Geiger-Nuttall law in nuclei is illustrated within the framework of Brown systematics, $\log T_\alpha$ *vs.* $Z_d^{(0.6)} Q_\alpha^{-1/2}$. This paper will present some of recent results in both structure and reaction studies, and will focus on the issues currently of interest along with possible directions for future experimental and theoretical advances in α-decay properties.

Key words: Super heavy nuclei (SHN), α-decay, α-clustering and scattering amplitudes, incoming/outgoing wave boundary conditions, resonance tunneling, decay-rates systematics.

PACS: 25.70.Jj, 27.90.+b.

1. INTRODUCTION

Both the amount and quality of the experimental data of fusion cross sections and the properties of nuclear energy levels of superheavy nuclei (SHN) have increased strongly over the last decade [1–12].

Analyzing the α-decay decay data found in literature, following important aspects emerged:
(*i*) α-decay rates exhibit an exponential dependence (Geiger-Nuttall) on emission energy; (*ii*) The ratio of α-hindrance factors for the odd-odd and even-even emitters is of about two orders of magnitude; (*iii*) Fine structure in the daughter nucleus is populated up to a few hundred of KeV.

For many SHN α-decay is the main and only observed decay mode and long α-decay chains usually terminate by the spontaneous fission (SF). Also, α-decay rates suffer large variations for transitions across the magic shells appearing inhibited by angular momentum and nuclear structure changes.

The physics of SHN is extremely rich and has produced key experiments facing the quest of shell structure with its manifestation in single particle and collective modes, radioactive states as multi-particle (multi-hole) excitations and high multipole transitions, producing long lived states, deformations and shape coexistence. It is a challenge to interpret the existing decay-data with theoretical models in order to better understanding the complex nuclear structure phenomena and reaction mechanisms behind.

Spontaneous decay observation of SHN into different fragments suggests a possible existence of different cluster structures in nuclei. Nuclear structure manifests itself in two typical structures identified in wide range of heavy and super-heavy nuclei, namely, clustering and fine structure. For many nuclei an α-particle appears as possible building block because of it very stable and inert behavior due to strong binding of two protons and two neutrons. The presence of α-cluster structure in SHN is suggested by the well developed cluster states with nα linear-chain structure and by the behavior of many SHN as continuous sources of α-particles.

In order to investigate these structures, a considerable theoretical work based on nuclear shell models and self-consistent mean field models has been carried out. Despite this effort, however, some important problems need to be solved:
(*i*) The masses of nuclei close to proton drip-line must be explored over large areas by performing new high-precision measurements and more accurate predictions for a better understanding of the nuclear fine structure as well as shell closures.
(*ii*) The uncertainties involved in locations of the proton single-particle (s.p.) energies for Z=114 to 126 should be eliminated;
(*iii*) Currently we have only a qualitative understanding for the competition α-SF based on simple schematic models. The study of many channel competition is ongoing and recent experiments are still under analysis, but number of promising results were already obtained, a few of which is will be mentioned in what follows.

This work is organized as follows. In Sec. 2 we give the necessary theoretical background for the calculation of α-decay rates. These calculations represent a refinement over previously and recently published work [16] based on the self-consistent nuclear models for the α-clustering and scattering amplitudes. The results, their systematics and comparison to α-decay data are presented in Sec. 3. Our work is summarized in Sec. 4.

2. ESTIMATES OF α-HALF-LIVES

2.1. THEORETICAL METHOD

In Ref. [13] the cluster decay width was expressed through the clustering and scattering amplitudes, and the decay rate problem was reduced to solving the eigen-

functions and eigenvalues of the Schrödinger equation associated to the decay process from different states [14–17]. The usual quantum mechanical rules for normalizations, orthogonality and completeness have to be extended in a straightforward manner in order to take into account the bound and scattering wave functions as well. In case of the α-decay of a single resonance state k into a single decay channel n, the α-half time is [13]:

$$T_n^k = ln2 \cdot \hbar/\Gamma_n^k \tag{1}$$

where, the decay width is

$$\Gamma_n^k = 2\pi \left| \frac{\int_{r_{min}}^{r_{max}} I_n^k(r) u_n^0(r) dr}{\int_{r_{min}}^{r_{max}} I_n^k(r) u_n^k(r) dr} \right|^2 . \tag{2}$$

In Eq.(6), $I_n^k(r)$ is the particle (cluster) formation amplitude (FA) defined as the antisymmetrized projection of the parent wave function (WF) $\mid \Psi_k >$ on the channel WF $\mid n\rangle = \mid [\Phi_D(\eta_1)\Phi_p(\eta_2)Y_{lm}(\hat{r})]_n\rangle$:

$$I_n^k(r) = r\langle \Psi_k \mid \mathcal{A}\left\{ [\Phi_D(\eta_1)\Phi_p(\eta_2)Y_{lm}(\hat{r})]_n \right\}\rangle \tag{3}$$

where $\Phi_D(\eta_1)$ and $\Phi_p(\eta_2)$ are the internal (space-spin) wave functions of the daughter nucleus and of the particle, $Y_{lm}(\hat{r})$ is the wave function of the angular motion, $\mathcal{A}$ is the inter-fragment antisymmetrizer, r connects the centers of mass of the fragments, and the symbol $<|>$ means integration over the internal coordinates and angular coordinates of relative motion.

In order to evidence the spectroscopic dependence of the emission rate, we shall use the standard nuclear shell model with harmonic oscillator s.p. wave functions coupled in a j-j representation. Here, following [18,19] we use the w.f. $\mid \Psi_k^{SM}(r_i)\rangle = \det \parallel \psi_{nlj}^{SM}(r_i) \parallel$, $i = 1, A$ and $\mid \Phi_D^{SM}\rangle = \det \parallel \psi_{nlj}^{SM}(\eta_{1i}) \parallel$, $i = 1, A-4$; and the α-particle wave function is chosen as:

$$\Phi_\alpha(\eta_2) = (2/(1/2)!)^{3/2}(\beta/\pi)^{9/4}(\rho_1^2+\rho_2^2+\rho_3^2)(4\pi)^{-3/2}\chi_{00}(s_1s_2)\chi_{00}(s_3s_4), \tag{4}$$

where the α-particle oscillator parameter is $\beta = 0.484$ fm^{-2}, χ_{00} is the singlet spin function and the internal spatial coordinates $\rho_1 = (r_1 - r_2)/\sqrt{2}$, $\rho_2 = (r_3 - r_4)/\sqrt{2}$, $\rho_3 = (r_1 + r_2 - r_3 - r_4)/2$, are connected to the individual coordinates r_i of the four nucleons. Replacing these functions in Eq. (6) we get

$$I_n^{k[SM]}(r) = r\langle \Psi_k^{SM}(r_i) \mid \mathcal{A}\left\{ \left[\Phi_D^{SM}(\eta_1)\Phi_p(\eta_2)Y_{lm}(\hat{r})\right]_n \right\}\rangle. \tag{5}$$

To perform the integrations in Eq. (5) we need to transform the w.f. $\Psi_k^{SM}(r_i)$ from the individual coordinates $(r_i) \longrightarrow r$, η_1, η_2, to the r_{CM} and internal coordinates η_1, η_2 of the fragments. Further, by integrating over the internal coordinates and the angular coordinates of the relative motion of fragments, the overlap integral is easily obtained in a compact form [18, 19].

2.2. EMPIRICAL METHODS

The radioactive decay law, according to which the probability to find the nucleus in the radioactive state decreases exponentially with the time, was formulated empirically by Geiger and Nuttall [20]. This was the observation that the experimental values of $\log T_\alpha$ plotted *vs.* $\mathrm{Q}_\alpha^{-1/2}$, where Q_α is the α-decay energy, fall on straight lines for the isotopes of a given element. Gamow [21] and independently Gurney and Condon [22] have solved the one body problem of the α-decay and derived the known Geiger-Nuttall relation from first principles of quantum mechanics. An explicit functional dependence of the halftime on the energy Q_α and on the proton number of daughter nucleus Z_d was introduced later in formulations [23, 24].

Here we consider two phenomenological formulas. The first is the Viola-Seaborg formula [23] which writes as

$$\log T_\alpha(s) = (aZ_d + b)Q_\alpha^{-1/2} + (cZ_d + d) + h_{e-o}, \tag{6}$$

where Q_α is the decay energy in MeV units, Z_d is the charge number of daughter nucleus; a,b,c,d are parameters and h_{e-o} is an even-odd hindrance term [25]. The parameters used are: a=1.66175; b=-8.5166; c=-0.20228; d=-33.9069, $h_{e-o} = 0.0$ (Z=even, N=even); $h_{e-o} = 0.772$ (Z=odd, N=even); $h_{e-o} = 1.066$(Z=even, N=odd); $h_{e-o} = 1.114$ (Z=odd, N=odd).
The second one is the Brown formula [24] given as

$$\log T_\alpha(s) = 9.54 Z_d^{(0.6)} Q_\alpha^{-1/2} - 51.37 + h_{e-o}. \tag{7}$$

The effective decay energy used in the above equations is

$$Q_\alpha = (A/(A-4))E_\alpha^{exp} + [6.53Z_d^{7/5} - 8.0Z_d^{2/5}]10^{-5}, \tag{8}$$

where, A is the mass number of the parent nucleus, E_α^{exp} is the measured kinetic energy of α-particle, and the second term is the screening correction [26].

Eq.(7) was tested for 119 data points (T_α, Q_α) (in a range of even Z_d from 74 to 106), all these points falling on a nearly universal line which represents the best linear fit to data [24].

3. RESULTS AND DISCUSSION

3.1. α-DECAY CHAINS OF $^{286}114$ AND $^{282}113$ NUCLEI

Tables 1 and 2 and Figures 1 and 2 present the known α-decay data for these nuclei and their descendants [2, 5] while, Tables 1 and 2 include the α-half-lives calculated theoretically: T^{SM} (Shell Model, Eqs.(1-5)), and empirically: T_α^{VS} (Viola-Seaborg, Eq.(6)) and T_α^B (Brown, Eq.(7)).

The results from Tables 1 and 2 may be summarized as follows:
1) Calculated values T_α^{SM} including even-odd corrections h_{e-o} have been found to provide an excellent description of the experimental data.
2) Almost a constant ratio T_α^{SM} / T_α^{VS}, suggests an increased stability due to shell structure.
3) T_α^{exp} is always in between our limit estimations [15] $T_\alpha^{SM} > T_\alpha^{exp} > T_\alpha^{res}$, where T_α^{res} represents the one-body half-time.
4) Values T_α^{SM} + h_{e-o} are in good agreement to empirical estimates T_α^{VS} and T_α^{B}.

Tables 1 and 2 also shows that the all calculated T_α-value decreases as Q_α increases, accordingly to the Geiger-Nuttall law.

3.2. SYSTEMATICS OF α-HALF-LIVES

The radioactive decay law, according to which the probability to find the nucleus in the radioactive state decreases exponentially with the time, was formulated empirically by Geiger and Nuttall [20]. This was the observation that the experimental values of $\log T_\alpha$ plotted *vs.* $Q_\alpha^{-1/2}$, where Q_α is the α-decay energy, fall on straight lines for the isotopes of a given element. Gamow [21] and independently Gurney and Condon [22] have solved the one body problem of the α-decay and derived the known Geiger-Nuttall relation from first principles of quantum mechanics. An explicit functional dependence of the halftime on the energy Q_α and on the proton number of daughter nucleus Z_d was introduced later in formulations [23, 24].

3.2.1. Experimental α-half-lives

The earliest systematics of α-decay lifetimes of naturally emitters was obtained [20] by plotting the experimental values of $\log T_\alpha$ *vs.* $Q_\alpha^{-1/2}$. Such a plot in Fig. 3 for observed transitions of SHN reveals a very smooth behavior for a given element Z with remarkable little scatter. Also note that the order of these lines is from large to small Z_d values.

As previously suggested [14, 16, 24, 27, 28] $\log T_\alpha$ *vs.* $Z_d Q_\alpha^{-1/2}$ may be a better way to plot the data. The result of this plot is shown in Fig. 4, where the data again form lines for a fixed Z_d value, and where the scatter from these lines is somewhat smaller than in Fig. 1. Now, we point out that the order of these lines is from small to large Z_d values being reversed in relation to the line $Z_d = 108$ which corresponds to a proton magic shell.

An interesting interpolation between Fig. 3 and Fig. 4 was argued and proposed for even-even heavy [24] by plotting $\log T_\alpha$ *vs.* $Z_d^{0.6} Q_\alpha^{-1/2}$. This interpolation extended to all known SHN is shown in Fig. 5, where the experimental points are falling on nearly universal straight lines which correspond to different (Z_d, N_d) parities. Fig.5 shows an important scatter of data points from these lines with relative

large standard errors (rms values)and therefore, we may conclude that the accuracy of known half-time measurements is roughly limited to an one order of magnitude.

3.2.2. Theoretical (Shell Model) α-half-lives

Figs. 6-8 present (in the same plots used in Figs. 3-5) theoretical (Shell Model) α-half-lives including even-odd corrections h_{e-o}. As we can see theoretical results reproduce very well the experimental results in different plots.

In spite of the same trend observed for the best fit lines in Figs.5 and 8, the scatter from these lines in Fig.8 appears reduced in comparison to the scatter from Fig.5. The very large scatter in Fig.5 may be indicate large errors in $\log T_{\alpha}^{exp}$ values.

Tables 1 and 2 resume the analysis of two channels measured recently [2, 5] using the SM approach and the empirical formulas [23,24]. We can observe in Tables 1 and 2 very close values for $\log T_{\alpha}^{SM} + h_{e-o}$ and $\log T_{\alpha}^{VS}$. The proposed best fit lines in Figs. 5 and 8 can be useful in the charge-energy detection of new α-emitters in the superheavy region.

3.2.3. Other approximations for α-half-lives

Simple resonance "one body" formulas for alpha half-time (T_{α}^{res}) have been used in Refs. [28–33] in spirit to papers [34, 35]. The approximate constant ratio $T_{\alpha}^{res}/T_{\alpha}^{SM}$ (see Table 1) ranging from 10^{-1} to 10^{-2} gives a measure of the contribution of the shell structure effects and of the nucleon finite size effects to the α-half-lives [15]. These effects lead to increasing of the α-half-lives. Also, these effects are contained implicitly in used experimental Q_{α}^{exp}-values which remain essential factors in determining the α-half-lives. Other interesting treatments of α-rates are described in detail in Refs. [36–39].

4. SUMMARY AND OUTLOOK

We have investigated the systematics of α-half-lives for SHN as predicted by theoretical self-consistent models for clustering and resonance scattering and by representative phenomenological models. The major influence of the pairing, resonance continuum, deformed shell closures, resonance scattering, and screening corrections was evidenced and provides a convenient basis for the interpretation of observed trends of the data and for prediction of new results.

The following conclusions can be drawn from our study:

1) The accuracy of known half-lives measurements is roughly limited to an one order of magnitude. The large discrepancies between experimental (Fig.5) and theoretical (Fig. 8) results could indicate wrong data and might be eliminated by improving accuracy of new measurements.

2) Systematic studies of nuclei from long α-decay chains across the major shell-closures are providing stringent new tests of our understanding about the microscopic structure of radioactive states.

3) The Brown systematics ($\log T_\alpha$ *vs.* $Q_\alpha^{-1/2}$) appears as a very useful tool in the study of α emitters in the superheavy region.

4) The very small widths of α-resonances observed experimentally in fusion- evaporation reactions, may be interpreted as resonance levels of radioactive products, and such a connection contributes directly to the study of the nuclear structure on the basis of decay data.

Table 1.

Experimental [2] and calculated α-half-lives for several SHN observed in element-114 decay chains.

Elem.	E_α^{exp} (MeV)	Q_α (MeV)	$\log T_\alpha^{exp}$ (s)	$\log T_\alpha^{SM}$ (s)	$\log T_\alpha^{VS}$ (s)	$\log T_\alpha^{B}$ (s)
^{286}114	10.310	10.507	-1.278	-1.151	-1.143	-1.129
^{281}Cn	10.310	10.507	-1.013	-0.706	-0.702	-0.575
^{277}Ds	10.570	10.771	-2.245	-1.990	-1.988	-1.661
^{273}Hs	9.590	9.778	-0.620	-0.017	-0.014	0.072
^{269}Sg	8.570	8.744	2.108	2.406	2.411	2.232

Table 2.

Experimental [5] and calculated α-half-lives of ^{282}113 and its daughters.

Elem.	E_α^{exp} (MeV)	Q_α (MeV)	$\log T_\alpha^{exp}$ (s)	$\log T_\alpha^{SM}$ (s)	$\log T_\alpha^{VS}$ (s)	$\log T_\alpha^{B}$ (s)
^{282}113	10.620	10.821	-1.210	-1.156	-1.153	-0.962
^{278}Rg	10.690	10.893	-2.367	-1.939	-1.937	-1.617
^{274}Mt	10.020	10.214	-0.485	-0.831	-0.829	-0.644
^{270}Bh	8.930	9.109	1.785	1.655	1.658	1.554

Interpretation	E (MeV)	Δt (s)	Pos (mm)
EVR—strip 28	15.97(4)		−1.0(2)
$^{285}114$ α decay	1.64(10)[a]	0.181	1.2(16)
^{281}Cn α decay	10.31(4)	0.140	−0.8(3)
^{277}Ds α decay	10.57(4)	0.008 21	−0.9(2)
^{273}Hs α decay	9.59(4)	0.346	−0.9(3)
^{269}Sg α decay	8.57(10)[b]	185	1.2(33)
^{265}Rf SF decay	208.1	152	−1.1(15)
EVR—strip 16	14.37(4)		−24.8(2)
$^{286}114$ α decay	10.31(10)[c]	0.0760	−20.4(39)
^{282}Cn SF decay	205.4	0.000 522	−22.5(15)

[a]Escape α particle depositing only partial energy in FPD.
[b]Reconstructed: 0.742 MeV in FPD and 7.823 MeV in UD.
[c]Reconstructed: 0.600 MeV in FPD and 9.705 MeV in UD.

Fig. 1 – Observed element-114 decay chains [2]. This table contains the times, energies, and positions of the two correlated decay chains observed in the experiment.

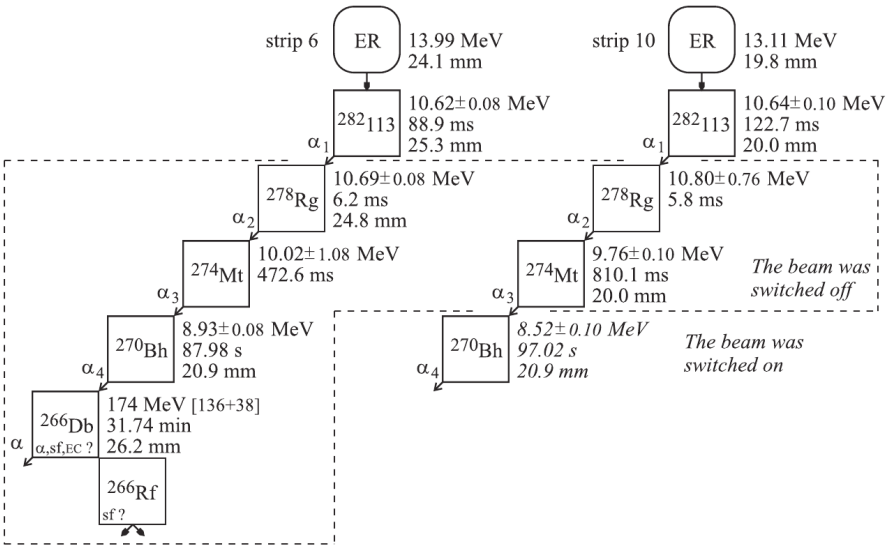

Fig. 2 – Time sequences in the decay chains of $^{282}113$ observed in the $^{237}Np+^{48}Ca$ reaction [5]. The measured α-particle energies, decay times, and positions of the observed events with respect to the top of the focal-plane detectors are shown.

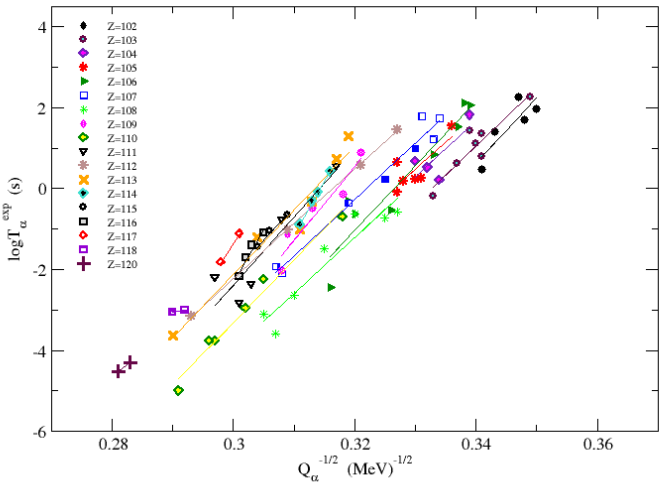

Fig. 3 – The experimental values of $\log T_\alpha^{exp}$ *vs.* $\mathrm{Q}_\alpha^{-1/2}$.

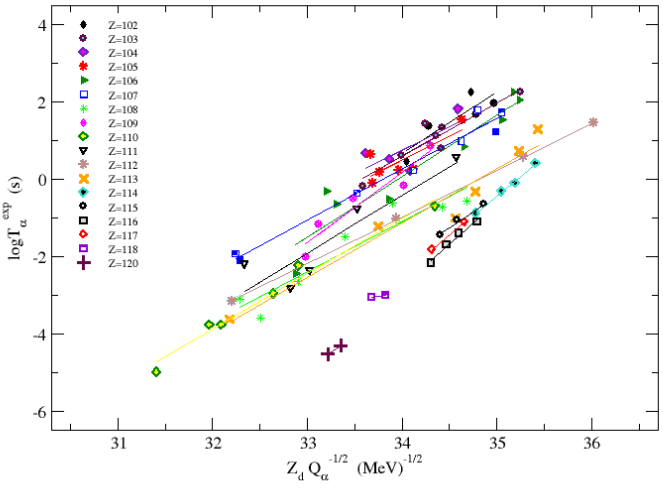

Fig. 4 – The experimental values of $\log T_\alpha^{exp}$ *vs.* $\mathrm{Z}_d\mathrm{Q}_\alpha^{-1/2}$.

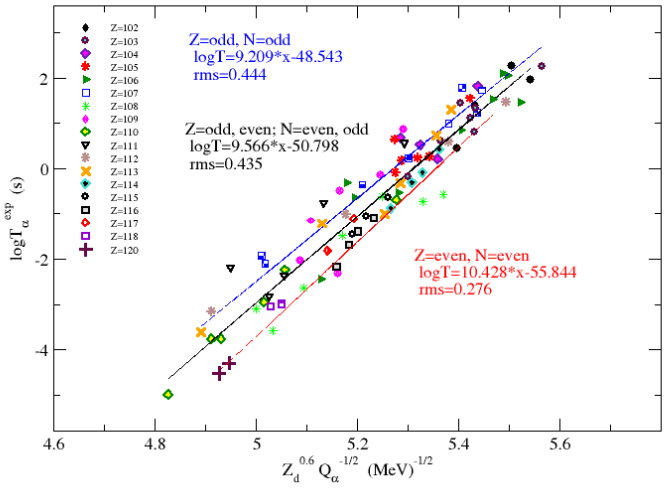

Fig. 5 – The values of $\log T_\alpha^{exp}$ (s) [1–7] are plotted *vs.* $Z_d^{0.6} Q_\alpha^{-1/2}$ for 88 data points. The straight lines represent the best fit to the all known T_α^{exp} values.

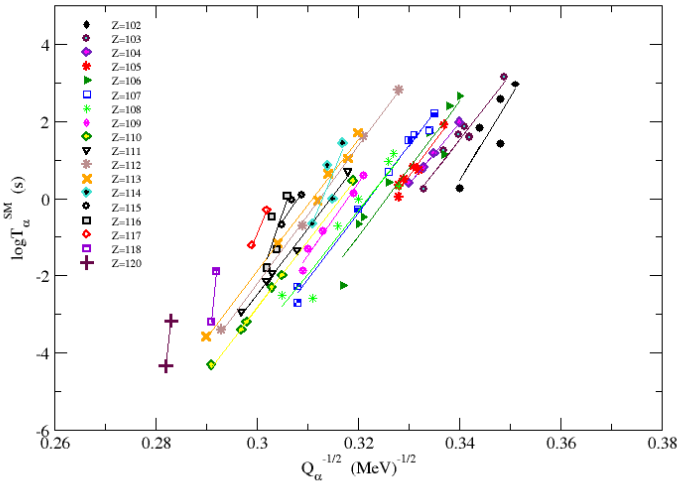

Fig. 6 – The values of $\log T_\alpha^{SM}$ *vs.* $\mathrm{Q}_\alpha^{-1/2}$.

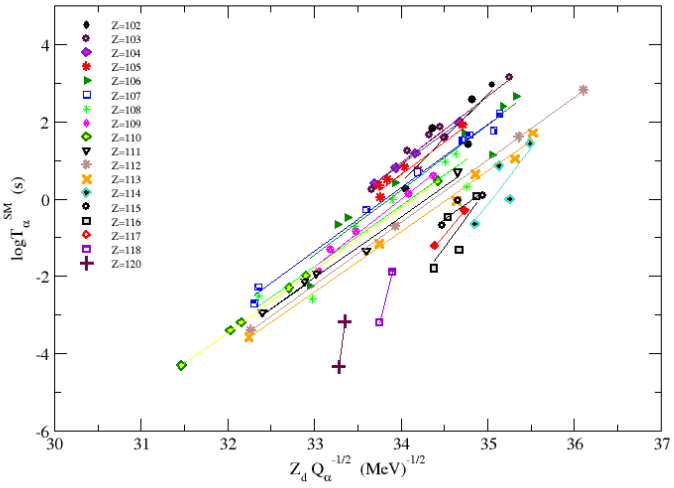

Fig. 7 – The values of $\log T_\alpha^{SM}$ *vs.* $Z_d Q_\alpha^{-1/2}$.

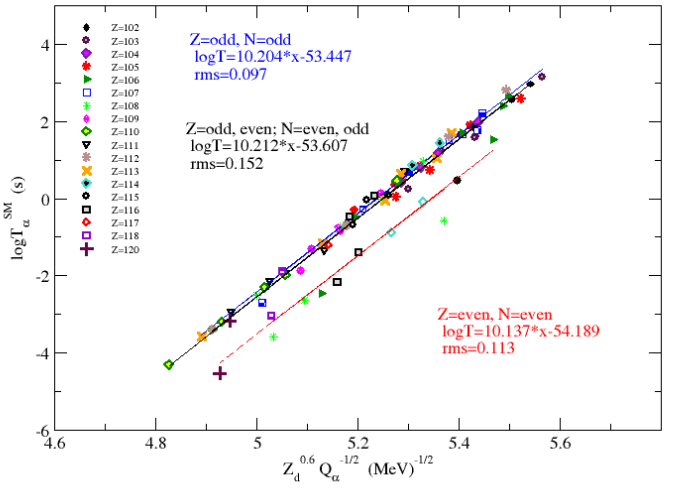

Fig. 8 – The values of $\log T_\alpha^{SM}$ (s) are plotted *vs.* $Z_d^{0.6} Q_\alpha^{-1/2}$ for 88 data points. The straight lines represent the best fit to the all known T_α^{exp} values.

Acknowledgments. We thank to Profs. Yu. Ts. Oganessian, V. K. Utyonkov, S. Hofmann, W. Scheid, A. Sandulescu, M. Rizea, Dr. Hab. S. Mişicu, and V. Grecu for many stimulating discussions. This work was supported from Contract: PN II 55/05.10.2011 and PN 09 37 01 02.

REFERENCES

1. Yu. Ts. Oganessian *et al.*, Phys. Rev. Lett. **104**, 142502 (2010).
2. P. A. Ellison, K. E. Gregorich, J. S. Berryman *et al.*, Phys. Rev. Lett. **105** 182701 (2010).
3. Ch. E. Düllmann *et al.*, Phys. Rev. Lett. **104**, 252701 (2010).
4. Yu. Ts. Oganessian *et al.*, Phys. Rev. C **79**, 024603 (2009).
5. Yu. Ts. Oganessian, V. K. Utyonkov, Yu. V. Lobanov *et al.*, Phys. Rev. C **76**, 011601(R) (2007).
6. Yu. Ts. Oganessian, J. Phys. G: Nucl. Part. Phys. **34**, R165R242 (2007).
7. Yu. Ts. Oganessian, Pure. Appl. Chem. **78**, 889 (2006).
8. J. Dvorak, W. Bruchle, M.Chelnokov *et al.*, Phys. Rev. Lett. **97**, 242501 (2006).
9. K. Morita, K. Marimoto, D. Kaji *et al.*, Jap. Phys. Soc. J. **73**, 2593 (2004).
10. S. Hofmann *et al.*, Eur. Phys. J. A **14**, 147 (2002).
11. S. Hofmann and G. Münzenberg, Rev. Mod. Phys. **72**, 733 (2000).
12. S. Hofmann *et al.*, Zeit. Phys. A **354**, 229 (1996).
13. I. Silişteanu , W. Scheid and A. Săndulescu, Nucl. Phys. A **679**, 317 (2001).
14. A. I. Budaca and I. Silişteanu, Rom. Rep. Phys. **63**, 1147-1166 (2011).
15. I. Silişteanu and A. I. Budaca, At. Data Nucl. Data Tables, (2012) in print.
16. I. Silişteanu, A. I. Budaca, A. O. Silişteanu, Rom. J. Phys. **55**, 1088 (2010).
17. V. Ledoux, M. Rizea, M. Van Daele, G. Vanden Berghe *et al.*, J. Comput. App. Math. **228**, 197-211 (2009).
18. H. J. Mang, Phys. Rev. **119**, 1069 (1960).
19. H. J. Mang, J. O. Rasmussen, Kgl. Danske Videnscab Selskab. Mat. Fys. Skifter **2**, 3 (1962).
20. H. Geiger and J. M. Nuttall, Philos. Mag. **22**, 613 (1911).
21. G. Gamow, Z. Physik **51**, 204 (1928).
22. R. W. Gurney and E. U. Condon, Nature (London) **122**, 439 (1928).
23. V. E. Viola and G. T. Seaborg, J. Inorg. Nucl. Chem. **28**, 741 (1966).
24. B. Alex Brown, Phys. Rev. C **46**, 811 (1992).
25. A. Sobiczewski, Z. Patyk, S. Cwiok, Phys. Lett. **224**, 1 (1989); Z. Patyk and A. Sobiczewski, Nucl. Phys. A **354**, 229 (1996).
26. J. O. Rasmussen, *Alpha-, beta- and gamma-ray spectroscopy*, K. Siegbahn ed., **1**, 701 (North-Holland, Amsterdam, 1968).
27. A. I. Budaca, I. Silişteanu, A. O. Silişteanu and C. I. Anghel, AIP Proceedings **1304**, 344-348 (2010).
28. I. Silişteanu, A. I. Budaca, A. O. Silişteanu and C. I. Anghel, J. Adv. Res. Phys. **2**, 011101 (2011).
29. I. Silişteanu , M. Rizea , B. I. Ciobanu *et al.*, Rom. J. Phys. **53**, 1191 (2008).
30. I. Silişteanu, A. Neacşu , A. O. Silişteanu *et al.*, AIP Proceedings **972**, 505-510 (2008).
31. I. Silişteanu, Rom. J. Phys. **52**, 775 (2007).
32. I. Silişteanu, A. Sandru, A. O. Silişteanu *et al.*, Rom. J. Phys. **52**, 807-822 (2007).
33. I. Silişteanu , A. Neacşu , A. O. Silişteanu *et al.*, Rom. Rep. Phys. **59**, 1173-1192 (2007).
34. M. Ivascu, A. Săndulescu, I. Silişteanu, Rev. Roum. Phys. **32**, 549 (1987).
35. A. Săndulescu, I. Silişteanu, M. Rizea, Rev. Roum. Phys. **23**, 823 (1978).

36. M. Rizea and N. Cârjan, Rom. Rep. Phys. **60**, 27-44 (2008).
37. M. Mirea, D. S. Delion, A. Săndulescu, Rom. J. Phys. **55**, 39 (2010).
38. M. Mirea, R. C. Bobulescu, M. Petre, Rom. Rep. Phys. **61**, 645 (2009).
39. M. Mirea, L. Tassan-Got, Rom. J. Phys. **54**, 331 (2009).